

# Mode Matching Technique for Aperture Array Antenna

Jong W. Zeong and Hyo J. Eom

Department of Electrical Engineering and Computer Science

Korea Advanced Institute of Science and Technology

373-1, Guseong-dong, Yuseong-gu, Daejeon, Korea

Phone +82-42-869-3436, Fax +82-42-869-8036

E-mail : hjeom@ee.kaist.ac.kr

**Abstract** Electromagnetic wave radiation from an aperture array antenna with a finite thickness is investigated. The mode matching technique is used to obtain simultaneous equations. The presented formulation is suitable for analyzing the radiation from a rectangular aperture array antenna.

**Keywords** aperture, array, antenna, Fourier transform, mode matching technique

## 1 Introduction

Aperture antennas are basic radiating structures and their radiation characteristics have been extensively studied. Aperture array antennas find many practical applications in microwave and millimeter wave frequencies. In this paper, the mode matching technique [1,2] is used to study the radiation property of an aperture array antenna, which is excited by an electric point source. The formulation presented in this paper is a fast convergent series form, which is numerically efficient.

## 2 Field Representations

Consider electromagnetic radiation from an aperture array antenna. The problem geometry is shown in Fig. 1. For the ease of formulation, an infinitely large conducting flange is assumed at  $z = 0$ . On the infinitely large conducting flange, a finite number of rectangular apertures are present. Fig. 1. shows only two apertures

( $l = 1, 2$ ) for illustration. The y-oriented electric current  $\bar{J} = \hat{y}J\delta(x')\delta(y')\delta(z')$  is in region (I), where  $\delta(\cdot)$  is the Dirac delta function. Region (I) is a three-dimensional rectangular cavity that is surrounded by PEC walls. Region (II) denotes the thick rectangular apertures. Region (III) denotes the upper half space ( $z > 0$ ). The total field in region (I) consists of the incident and scattered components. It is convenient to use the magnetic and electric vector potentials,  $\bar{A}$  and  $\bar{F}$ , for field representations. The incident vector potential  $A_y^i$  results from the electric current  $\bar{J}$  as

$$A_y^i = \sum_{s=1}^{\infty} \sum_{t=1}^{\infty} -\frac{\mu_0 J}{\kappa_1 \sin(\kappa_1 d)} \times \Psi_s(x')\Psi_s(x)\Phi_t(y')\Phi_t(y) \times \begin{cases} \sin \kappa_1(z' + t + d) \sin \kappa_1(z + t) \\ \phantom{\sin \kappa_1(z' + t + d)} z' < z < -t \\ \sin \kappa_1(z' + t) \sin \kappa_1(z + t + d) \\ \phantom{\sin \kappa_1(z' + t)} -t - d < z < z' \end{cases} \quad (1)$$

where  $\Psi_s(x) = \sqrt{\frac{1}{\alpha}} \sin \alpha_s(x + \alpha)$ ,  $\Phi_t = \sqrt{\frac{1}{\beta}} \cos \beta_t(y + \beta)$ ,  $\alpha_s = \frac{s\pi}{2\alpha}$ ,  $\beta_t = \frac{t\pi}{2\beta}$ ,  $\kappa_1 = \sqrt{k_o^2 - \alpha_s^2 - \beta_t^2}$ .

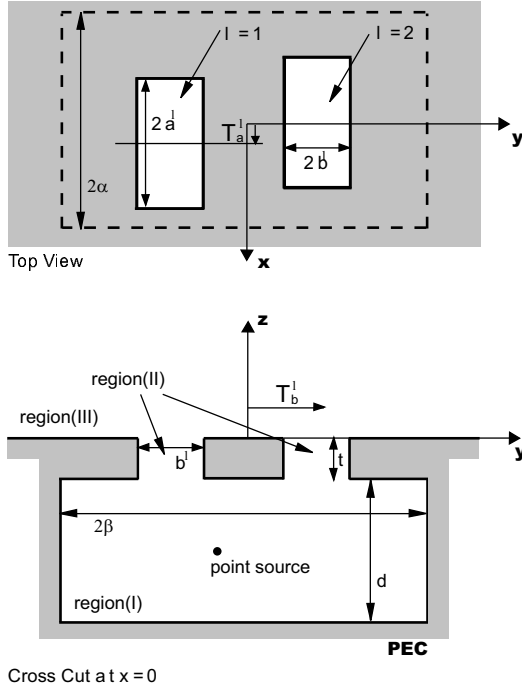


FIG. 1: Problem geometry

The scattered vector potentials in region (I) are assumed to be

$$F_z^s(x, y, z) = \sum_{g=0}^{\infty} \sum_{j=0}^{\infty} e_{gj} \sin \gamma_{gj} (z + t + d) \times \cos \alpha_g (x + \alpha) \cos \beta_j (y + \beta) \quad (2)$$

$$A_z^s(x, y, z) = \sum_{g=1}^{\infty} \sum_{j=1}^{\infty} \bar{e}_{gj} \cos \gamma_{gj} (z + t + d) \times \sin \alpha_g (x + \alpha) \sin \beta_j (y + \beta) \quad (3)$$

where  $(g, j) \neq (0, 0)$ ,  $\alpha_g = \frac{g\pi}{2\alpha}$ ,  $\beta_j = \frac{j\pi}{2\beta}$ , and  $\gamma_{gj} = \sqrt{k_o^2 - \alpha_g^2 - \beta_j^2}$ .

The vector potentials in regions (II) and (III) are written as

$$F_z^{II} = \sum_{m=0}^{\infty} \sum_{n=0}^{\infty} \cos a_m^l (x - T_a^l + a^l) \times \cos b_n^l (y - T_b^l + b^l) \times [C_{mn}^l \cos \xi_{mn}^l (z + t) + D_{mn}^l \sin \xi_{mn}^l (z + t)] \quad (4)$$

$$A_z^{II} = \sum_{m=1}^{\infty} \sum_{n=1}^{\infty} \sin a_m^l (x - T_a^l + a^l) \times \sin b_n^l (y - T_b^l + b^l) \times [\bar{C}_{mn}^l \cos \xi_{mn}^l (z + t) + \bar{D}_{mn}^l \sin \xi_{mn}^l (z + t)] \quad (5)$$

where  $a_m^l = \frac{m\pi}{2a^l}$ ,  $b_n^l = \frac{n\pi}{2b^l}$ , and  $(\xi_{mn}^l)^2 = k_o^2 - (a_m^l)^2 - (b_n^l)^2$ .

$$F_z^{III} = \frac{1}{(2\pi)^2} \int_{-\infty}^{\infty} \int_{-\infty}^{\infty} \tilde{F}_z^{III}(\zeta, \eta) \times e^{-i\zeta x - i\eta y + i\kappa z} d\zeta d\eta \quad (6)$$

$$A_z^{III} = \frac{1}{(2\pi)^2} \int_{-\infty}^{\infty} \int_{-\infty}^{\infty} \tilde{A}_z^{III}(\zeta, \eta) \times e^{-i\zeta x - i\eta y + i\kappa z} d\zeta d\eta \quad (7)$$

where  $\kappa = \sqrt{k_o^2 - \zeta^2 - \eta^2}$ . Note that  $\tilde{F}_z^{III}(\zeta, \eta)$  and  $\tilde{A}_z^{III}(\zeta, \eta)$  are given by

$$\tilde{F}_z^{III}(\zeta, \eta) = \int_{-\infty}^{\infty} \int_{-\infty}^{\infty} F_z^{III}(x, y, 0) e^{i\zeta x + i\eta y} dx dy$$

$$\tilde{A}_z^{III}(\zeta, \eta) = \int_{-\infty}^{\infty} \int_{-\infty}^{\infty} A_z^{III}(x, y, 0) e^{i\zeta x + i\eta y} dx dy$$

### 3 Enforcement of Boundary Conditions

In order to determine the unknown modal coefficients  $C_{mn}^l, D_{mn}^l, \bar{C}_{mn}^l$ , and  $\bar{D}_{mn}^l$ , we enforce the boundary conditions on  $E_{x,y}$  and  $H_{x,y}$  at  $z = 0$  and  $-t$ . Applying the Fourier transform to the  $E_{x,y}$  field continuities at  $z = 0$ , we get  $\tilde{F}_z^{III}(\zeta, \eta)$ ,  $\tilde{A}_z^{III}(\zeta, \eta)$  in terms of  $C_{mn}^l, D_{mn}^l, \bar{C}_{mn}^l$ , and  $\bar{D}_{mn}^l$ . The continuities of tangential magnetic fields at  $z = 0$  over the apertures are necessary for further simplification. Substituting  $\tilde{F}_z^{III}(\zeta, \eta)$  and  $\tilde{A}_z^{III}(\zeta, \eta)$  into the  $H_{x,y}$  field continuities and performing algebraic manipulation gives the simultaneous equations for  $C_{mn}^l, D_{mn}^l, \bar{C}_{mn}^l$  and  $\bar{D}_{mn}^l$ . We note that the mode matching technique based on the sinusoidal orthogonality must be used in

the algebraic manipulation. The final equations, which can be obtained from the boundary conditions at  $z = 0$ , are

$$\begin{aligned}
& \frac{(a^l b^l a^r b^r)^2}{4\pi^2} a_p^r \sum_{l=1}^N \sum_{m=0}^{\infty} \sum_{n=0}^{\infty} \\
& \times \left( C_{mn}^l \cos \xi_{mn}^l d + D_{mn}^l \sin \xi_{mn}^l d \right) \\
& \times \left\{ \omega (a_m^l)^2 I_{mnpq}^{(2)lr} - \frac{(a_m^l)^2 + (b_n^l)^2}{\omega \mu_o \epsilon_o} I_{mnpq}^{(1)lr} \right\} \\
& + \frac{i(a^l b^l a^r b^r)^2}{4\pi^2 \mu_o} a_p^r \sum_{l=1}^N \sum_{m=1}^{\infty} \sum_{n=1}^{\infty} a_m^l b_n^l \xi_{mn}^l \\
& \times \left( \bar{C}_{mn}^l \sin \xi_{mn}^l d - \bar{D}_{mn}^l \cos \xi_{mn}^l d \right) I_{mnpq}^{(2)lr} \\
& = \frac{i}{\omega \mu_o \epsilon_o} a_p^r \xi_{pq}^r \left( C_{pq}^r \sin \xi_{pq}^r d - D_{pq}^r \cos \xi_{pq}^r d \right) \\
& \quad \times \delta_{mp} \delta_{nq} \delta_{lr} \epsilon_q a^r b^r \\
& + \frac{1}{\mu_o} b_q^r \left( \bar{C}_{pq}^r \cos \xi_{pq}^r d + \bar{D}_{pq}^r \sin \xi_{pq}^r d \right) \\
& \quad \times \delta_{mp} \delta_{nq} \delta_{lr} a^r b^r
\end{aligned} \tag{8}$$

$$\begin{aligned}
& \frac{(a^l b^l a^r b^r)^2}{4\pi^2} b_q^r \sum_{l=1}^N \sum_{m=0}^{\infty} \sum_{n=0}^{\infty} \\
& \times \left( C_{mn}^l \cos \xi_{mn}^l d + D_{mn}^l \sin \xi_{mn}^l d \right) \\
& \times \left\{ \omega (b_n^l)^2 I_{mnpq}^{(3)lr} - \frac{(a_m^l)^2 + (b_n^l)^2}{\omega \mu_o \epsilon_o} I_{mnpq}^{(1)lr} \right\} \\
& - \frac{i(a^l b^l a^r b^r)^2}{4\pi^2 \mu_o} b_q^r \sum_{l=1}^N \sum_{m=1}^{\infty} \sum_{n=1}^{\infty} a_m^l b_n^l \xi_{mn}^l \\
& \times \left( \bar{C}_{mn}^l \sin \xi_{mn}^l d - \bar{D}_{mn}^l \cos \xi_{mn}^l d \right) I_{mnpq}^{(3)lr} \\
& = \frac{i}{\omega \mu_o \epsilon_o} b_q^r \xi_{pq}^r \left( C_{pq}^r \sin \xi_{pq}^r d - D_{pq}^r \cos \xi_{pq}^r d \right) \\
& \quad \times \delta_{mp} \delta_{nq} \delta_{lr} \epsilon_q a^r b^r \\
& - \frac{1}{\mu_o} a_p^r \left( \bar{C}_{pq}^r \cos \xi_{pq}^r d + \bar{D}_{pq}^r \sin \xi_{pq}^r d \right) \\
& \quad \times \delta_{mp} \delta_{nq} \delta_{lr} a^r b^r
\end{aligned} \tag{9}$$

where  $I_{mnpq}^{(1)lr}$  through  $I_{mnpq}^{(3)lr}$  are double integral representations. Computation are needed to evaluate the double integrals,  $I_{mnpq}^{(1)lr}$  through  $I_{mnpq}^{(3)lr}$ .

It is necessary to obtain another set of the simultaneous equation for  $C_{mn}^l$ ,  $D_{mn}^l$ ,  $\bar{C}_{mn}^l$  and  $\bar{D}_{mn}^l$ , by using the boundary conditions at  $z = -t$ . The simultaneous equations, which can be obtained from the boundary conditions at  $z = -t$ , are somewhat similar to (8) and (9); hence, we do not show their explicit expressions.

## 4 Computations

Using the stationary phase approximation, it is possible to evaluate the antenna radiation pattern. In order to check the validity of our computation, the numerical results of the antenna radiation patterns are compared with the CST MicroWave Studio results. The E- and H-plane radiation patterns for  $a^{1,2} = 3$  cm,  $b^{1,2} = 0.15$  cm,  $t = 1$  cm,  $\alpha = 6$  cm,  $\beta = 5$  cm,  $d = 19.4$  cm,  $(x', y', z') = (0, 0, -16.5)$  cm,  $T_a^1 = T_a^2 = 0$ ,  $T_b^1 = 3$  cm,  $T_a^2 = -3$  cm and  $f = 2.5$  GHz are shown in Fig. 2 and Fig. 3, respectively. The agreement between E-plane radiation patterns is better than that of H-plane. The number of modes used in our computation is  $m = n = 2$  and  $g = j = 3$ , thus indicating fast numerical convergence.

## 5 Conclusion

In this paper, we presented a rigorous formulation to investigate radiation from an aperture array antenna, which consists of multiple rectangular thick apertures. By using the Fourier transform and mode matching technique, we obtain a formulation in a fast convergent series form. Our computation results agree with others based on the numerical approach.

## Acknowledgment

This work was supported by KOSEF (Korea Science and Engineering Foundation) under the project (R01-2002-000-00189).

## References

- [1] H. H. Park and H. J. Eom, "Electromagnetic scattering from multiple rectangular apertures in a thick conducting screen," *IEEE Trans. Antennas Propagat.*, vol. 47, no. 6, pp. 1056-1060, June 1999.
- [2] H. H. Park and H. J. Eom, "Electromagnetic penetration into a rectangular cavity with multiple rectangular aperture in a conducting plane," *IEEE Trans. Electromagn. Compat.*, vol. 42, no. 3, pp. 301-307, Aug. 2000.

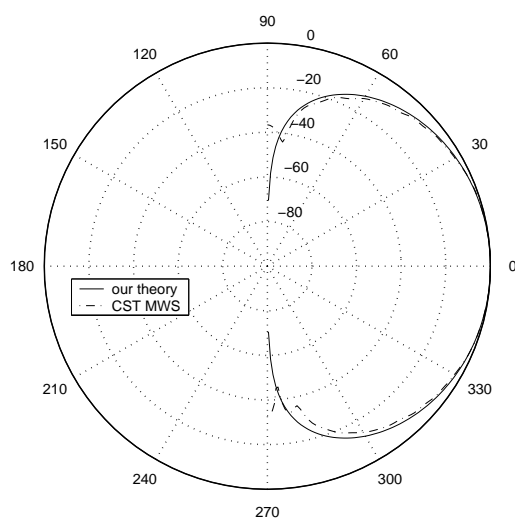


FIG. 2: E-plane ( $y - z$  plane) radiation pattern

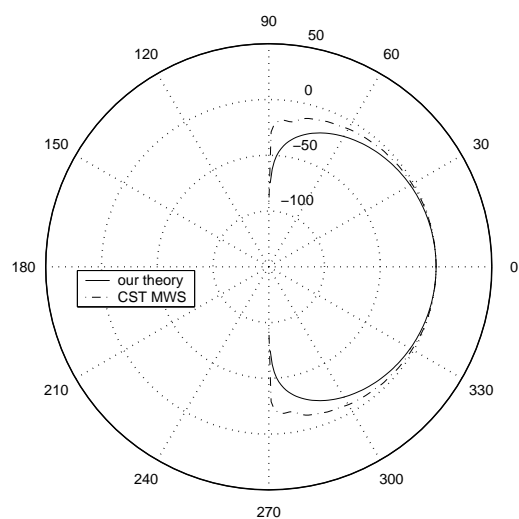


FIG. 3: H-plane ( $x - z$  plane) radiation pattern